ARTICLE

doi: 10.1059/nature15943

Optimal Chip Configuration for Multiplexed, Single Step, On Chip Mutation Detection in Circulating Tumor DNA Device

Shilpika Chowdhury[1], Taylor Lee[1], Ori Hoxha[1], Amanda Haack[1]

This paper discusses the development of an on chip, fully integrated device for detecting circulating DNA mutations indicating cancer treatment effectiveness from a patient blood sample. In this paper, we explore the various configurations needed to detect, process, and visualize a blood sample in a fully contained microfluidic unit. Specifically this work regards the optimization of the likelihood of detecting a mutation, the subsequent pre-concentration and allele-specific PCR wells, and the ultimate fluorescent visualization of the sample in the device. The important contributing factors were the minimization of the well thickness for uniform heating while preserving the fluorescent density of the overall device.

Non-small cell cancer treatment is a pervasive issue within the subset of patients suffering from lung cancer, the most common form of cancer. Of the patients who develop non-small cell lung cancer, many are diagnosed with unresectable tumors. A developing alternative in situations where a tumor cannot be surgically removed is the administration of oral drugs specifically targeting tyrosine kinase activity. These drugs, aptly named tyrosine kinase inhibitors, are effective in a fraction of patients that are genetically predisposed to respond to treatment. The gold standard approach for testing for mutations indicating compatibility is an invasive tumor biopsy, which can often only be collected very few times during treatment, and a subsequent shipment to a lab where the biopsy tissue is lysed, DNA is extracted, and the sample is tested for mutations.

A device developed by Hoxha *et al*[1] adopts a liquid biopsy, as a blood sample, for detection of circulating DNA mutation and an automated LOC device that completes the entire sample preparation, PCR circulating DNA amplification, and ultimate fluorescence detection of mutation presence. The described device is optimized for ideal mutation detection, rapid thermocycle time, and ideal optical configuration using computer simulation (COMSOL).

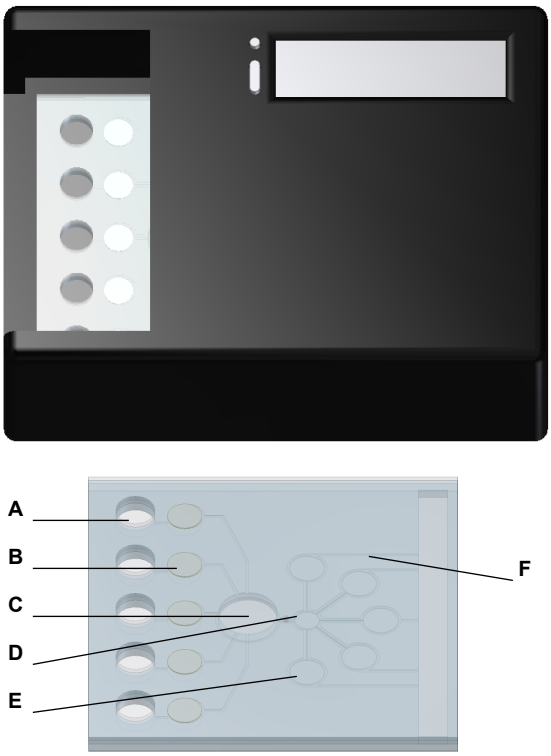

Figure 1 | CAD Model of Device Housing and Chip. A Device inlet **B** Filter separation **C** Pre-concentration PCR well **D** Magnetic Screw Valve **E** Allele-specific PCR well and fluorescent detection **F** degas capillaries. Chip begins on left side of device for thermocycling and is autonomously moved to right by housing unit for fluorescent detection.

Device Overview

The presented device is comprised of five inlet wells, a filter-on-top blood plasma separation scheme, pre-concentration PCR, allele-specific PCR, and an LED stimulated fluorescent detection. Blood is placed into the inlet wells after which the filter-on-top separation method, described by Lee *et al*[2], separates plasma with circulating DNA from large blood cells and proteins through sedimentation and filtration. The plasma is then deposited into a large pre-concentration PCR well where PCR reagents have been freeze-dried to the well floor. A Peltier thermocycler cycles the well between 95 °C and 60 °C in accordance with a rapidly annealing polymerase which mitigates the traditional PCR annealing step as described by Beer *et al*[3]. After pre-

concentration, the liquid moves to final wells for allele-specific amplification. Each well contains a combination of specific mutation primers, nucleotides, polymerase, as well as specific fluorescent labeling molecules (scorpion probes) for detection. After allele-specific PCR through Peltier thermocycling, the chip is moved autonomously within the housing unit to a fluorescence chamber where bound scorpion probes are exited to indicate the presence of mutations (Exon 19 deletion, G719X, L858R, Exon 20 insertion and T790M[4]). This signal is collected by a phototransistor digitally and is displayed on the device housing.

The entire device is comprised of a 0.25 mm base PMMA layer, a PDMS intermediate layer (patterned on both sides with 250 µm SU8 and pierced with well punches), and a fabricated PMMA cover. All channels are patterned in PDMS to allow for degas driven flow, enhanced using small capillaries around each well which are connected to the degas reservoir. All degas driven flow is implicit through the 50 µm walls around channels and wells that separate the fluid region from degas capillaries, rather than directly accessing the liquid.

Minimum Blood Volume for Detection

Minimum blood volume was determined using a worst-case approximation for occurrence of mutations, 3 mutations per 1 mL blood for Exon 19 deletion, G719X. All other tested mutations occur at higher frequency in the blood[4]. The filter-on-top efficiency of plasma separation from blood is expected to be roughly 40% of blood volume[2], resulting in 200 µL of plasma at pre-concentration (and 350 µL of blood at each of the 5 inlets). The 5 mutation testing chambers were limited to 10 µL, with only 60 µL total allowed to pass from pre-concentration to allele-specific PCR. Allele specific PCR wells can be optimized to hold less sample but are limited by fluorophore density, signal attenuation, and well geometry.

Degas Chamber Dimensions

While very little formal research has been done on degas driven flow, it is expected that a degas reservoir should be of at least a larger volume than the liquid that is expected to flow though. The total liquid expected to flow through the device was calculated neglecting transport channels (which all held less than 1 µL). The total inlet blood volume is roughly 2000 µL, resulting in the degas reservoir dimensions of 2 mm x 50 mm x 20 mm. In addition to pure volume, degas should also take into account the expected resistance to flow because the degas reservoir is not in direct contact with the fluidic channels. Therefore, a 2 mm x 60 mm x 30 mm degas reservoir is expected for optimal flow instigation in the device.

Peltier Thermocycling

Both the pre-concentration and allele specific PCR cycles were regulated using a Peltier thermocycler, a device that is capable of both heating and cooling. Thermocyclers can be programmed to have variable unit area wattage. COMSOL simulation was run to determine the ideal wattage that optimized both cycle length and well uniformity. In each well type, a single well is simulated as a circular disk filled with water surrounded by a 100 µm degas capillary, modeled as air. Between the capillary and the well is a 50 µm PDMS wall. The bottom and top of these are PMMA layers, 0.25 mm and 1 mm respectively. 0.25 mm PMMA was selected for the bottom layer thickness to allow for efficient thermal transmission without excessive heat buildup in the PMMA, which has a low melting point of 160 °C.

After a simulation with the highest heat flux available for standard Peltier devices, negligible change in temperature of the air above the model was observed due to the extremely low thermal conductivity of air above the channel. Therefore, the air component was left out of evaluation simulations

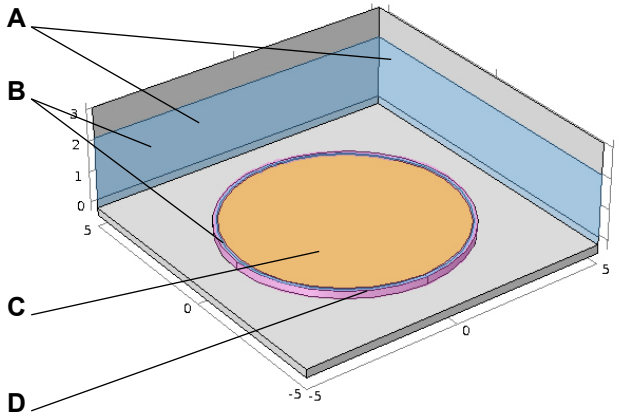

Figure 2 | Simulation Schematic. A PMMA top and bottom cover (gray) **B** PDMS intermediate layer (blue) **C** PCR Channel with Plasma (orange) and **D** Capillary degas with air (pink)

Material	α (m^2/s)	k (W/m K)	C (J/kg K)	ρ (kg/m^3)
Water	14.3e-4	0.563	4186	999.97
PDMS[10]	1.06e-7	0.15	1460	965
PMMA[11]	11.0e-7	0.25	1300	1683
Air	1.9e-5	0.024	1006	1.225

Table 1 | Simulation Parameters. Thermal Diffusivity (α), Thermal Diffusivity (k), Specific Heat (C), and Density (ϱ).

The well dimensions were first minimized for optimal heat transfer. Channel heights of 0.25 mm, 0.5 mm, 1 mm, and 2 mm were tested for a 25,000 W/m^2 heat flux at the base of the simulation. The selected thicknesses were based on sample containment requirements. This stage of testing hadn't yet optimized the thermocycler wattage and instead aimed to determine an effective well depth for uniformity and PMMA integrity. Simulations were run with the initial condition of 20 °C for all components because the initial heat-up step is most susceptible to heat buildup at the base of the device in the PMMA base layer.

Depth (mm)	ΔT (°C)	Time (sec)	Max. Temperature (°C)
0.25	3	2	162
0.5	6	6	186
1	11	28	212
2	23	193	264

Table 2 | Well Depth Simulation Results at 25,000 W/m². Table shows difference in temperature between top and bottom of the well, time to achieve average temperature, and maximum temperature of device (at base of PMMA bottom layer). Depth of 0.25 mm maximized uniformity and minimized cycle time. The maximum temperature was lowest, but flux was too high to prevent PMMA base layer from melting.

Simulation revealed that a depth of 0.25 mm is optimum for holding a sample of 10 μL as in the allele-specific PCR chambers. Table 2 shows the dependence of temperature uniformity, time for cycle leg completion, and maximum temperature at PMMA base later relative to well depth. A thinner channel increased uniformity, but would be suited for a smaller sample testing volume. For the pre-concentration PCR, which is executed on 200 μL of sample, is not space effective with a 0.25 mm depth (resulting in a 11 mm radius). Instead, a 0.5 mm depth with a loss in cycle brevity is more effective.

After determining the optimum thickness for each well, wattage simulation was done to determine the best balance between temperature uniformity and cycle time.

Pre-concentration PCR

Because pre-concentration PCR is executed only 15 times[1] in a large well, the ideal power density and cycle time differs from allele-specific PCR. Table 3 shows data from the initial heat up, cool down leg of the cycle, and heat up leg of the cycle in the pre-concentration well. The total ideal cycle time was 31 seconds. The optimal heat-up time was 61 seconds, the cool down cycle leg was 13 seconds and the heat-up cycle leg was 8 seconds, making each cycle 21 seconds long. Final time for PCR was less than 7 minutes.

As a result of simulations, the heat flux in the first leg is optimized at 6000 W/m² during initial heating for uniformity, -10,000 W/m² for cool down and 10,000 W/m² for heat up. The wattage and direction of the thermocycler can be regulated by the control box. The thermal uniformity in the well with these parameters was 4 °C on average among the cycle legs.

A

Flux (W/m²)	ΔT (°C)	Time (sec)	Max. Temperature (°C)
25000	40	12	198
21875	35	15	165
10000	20	29	154
8000	15	43	141
6000	**4**	**61**	**138**

B

Flux (W/m²)	ΔT (°C)	Time (sec)	Max. Temperature (°C)
-25000	7	5	0
-18750	4	6	13
-10000	**2**	**13**	**30**

C

Flux (W/m²)	ΔT (°C)	Time (sec)	Max. Temperature (°C)
25000	10	4	203
21875	8	6	189
10000	**4**	**8**	**152**
8000	2	13	143

Table 3 | Wattage Simulation Results in 0.5 mm Deep Well for Pre-concentration PCR Well. A heat up from room temperature time and uniformity **B** Cool down from 95°C to 60°C time and uniformity **C** Heat up from 60°C to 95°C.

Allele-Specific PCR

Allele specific PCR was determined to be optimized at 30 cycles for amplification of DNA in this device[1]. The optimized cycle length was 8 seconds, making the total time for PCR less than 5 minutes (4.75 min). Thermal uniformity in the channel was on average 1.5 °C over the cycles.

A

Flux (W/m²)	ΔT (°C)	Time (sec)	Max. Temperature (°C)
31250	9	6	167
25000	8	8	161
21875	6	10	161
18750	5	12	154
15625	**4**	**15**	**147**

B

Flux (W/m²)	ΔT (°C)	Time (sec)	Max. Temperature (°C)
-31250	3	2	5
-25000	2	3	15
-21875	**0.61**	**5**	**30**
-15625	0.4	8	35

C

Flux (W/m²)	ΔT (°C)	Time (sec)	Max. Temperature (°C)
31250	7	1	201
25000	5	1.7	184
21875	**2.25**	**3**	**142**
15625	1.5	5	138

Table 4 | Wattage Simulation Results in 0.25 mm Deep Well for Allele-Specific PCR Well. A heat up from room temperature time and uniformity. Heat-up is less uniform and longer in duration than other cycle components. **B** Cool down from 95°C to 60°C time and uniformity data, favoring time if uniformity is below 1 degree **C** Heat up from 60°C to 95°C data, favoring time over uniformity.

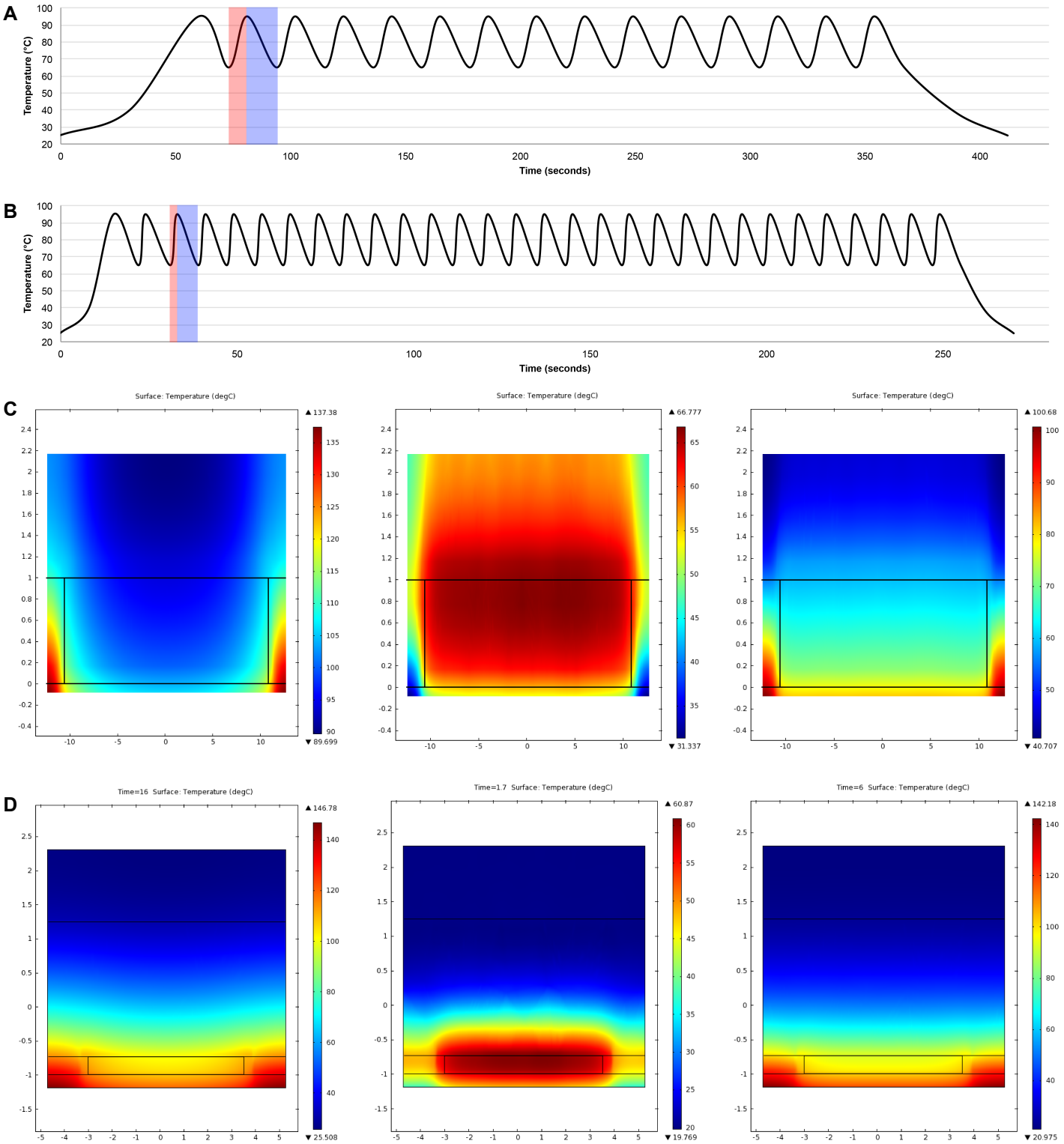

Figure 3 | Results from COMSOL Thermal Simulation. A Plot of thermal cycling for pre-concentration PCR. Heat up cycle leg was 8 seconds and cool down leg was 13 seconds. The total cycle length is 21 seconds with a total runtime for 15 cycles at about 7 minutes **B** Plot of thermal cycling for pre-concentration PCR. Heat up cycle leg was 8 seconds and cool down leg was 13 seconds. The total cycle length is 21 seconds with a total runtime for 15 cycles at about 7 minutes **C** Pre-concentration PCR simulation for initial heat up (61 s), cool down (13 s), and heat up (8 s) cycles from left to right **D** Allele-specific PCR simulation for initial heat up (15 s), cool down (5 s), and heat up cycles from left to right (3 s).

The PCR steps in the optimized device take a total of fewer than 12 minutes to perform, and flow between wells is very fast due to small channels connecting them. The only further limiting step is the filter-on-top plasma separation, which is expected to take roughly 15 minutes. The total device processing time from initial blood input until detection will be under 30 minutes. In comparison, simulations of the original device show a device run time of 50 minutes with the presented alternative geometries for heating and cooling cycles.

Optical Optimization

After amplification, even a very low circulating DNA blood sample should achieve saturation due to the number of PCR cycles (15 in pre-concentration, 30 in allele-specific). The saturation density during PCR in the well is therefore limited by reagents, the concentration of which is minimized to reduce primer cost per sample. This minimum concentration can be determined by optical simulation for detectability.

For the phototransistor to collect a reliable signal, at least 10^6 photons must enter the selected phototransistor (TT electronics OP805TXV-NDo)[5] through a cross sectional area of 17.72 mm^2 at the phototransistor lens, or 56,4000 photons/mm^2. Each fluorescent probe releases a single photon of light at 515 nm, requiring redirection into the phototransistor for detection. The optical attenuation of the PDMS is negligible. PDMS has a refractive index of about 1.4 and is transparent in the visible range (240 nm – 1100 nm) with an extinction coefficient of < 10^{-10}. PDMS also has negligible birefringence[6].

In order to be sensed by the phototransistor the signal must be bright enough or be redirected with an embedded lens. The fluorescent signal is based on the fluorescent scorpion probe density. Scorpion probe density is directly related to the number of DNA strands present, which should be limited only by available reagents. Upon detection of DNA, the probes will fluoresce when exposed to 500 nm light. The light then passes through the PDMA and PMMA layers or through lenses before being filtered for 500 nm and being detected by a phototransistor.

The phototransistor used in the device housing has a half angle of acceptance of 12° and is a fixed distance of 10 mm away from the base of the chip[7]. The consequence of those two factors results in a detection field of 2.12 mm in radius, which can only decrease if the detector is moved closer to the sample. The chamber LED is expected to fully illuminate the sample.

Detection feasibility can be quantified by taking into account the well depth and fluorophore density given the minimum photons/area for detection. The effective possible combinations are the green area in **Figure 4**.

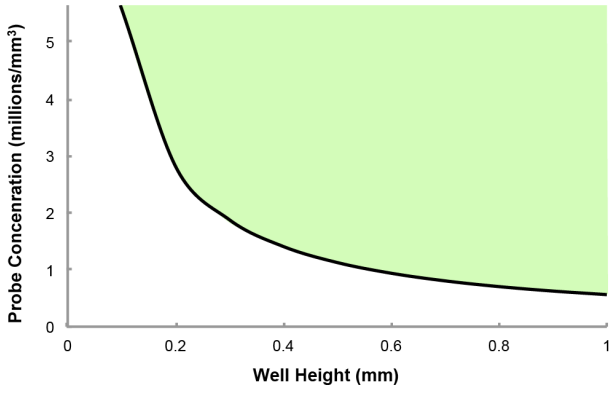

Figure 4 | Probe Concentration Plot. Required probe concentration based on a minimum photon density of 56,400 photons/mm^2. Green region contains all concentration-height pairs that are reliably detected.

At a channel height of 0.25 mm, the minimum probe density was found to be 2,256,000 molecules/mm^3, or 3.7 pM and 1,128,000 molecules/mm^3 (1.8 pM) at 0.5 mm, which is already very low.

In order to further reduce reagent use, it is possible to concentrate the signal by incorporating microlenses above the detection area as in **Figure 5A**. The lens will accept light from a large area, and concentrate all the collected photons at the back focal length. The back focal length of a possible microlens should be just longer than the distance to the phototransistor to achieve the strongest signal. The diameter (d) and sag (h) of the lens were selected as 100 mm and 12 mm respectively. The radius of curvature (R) is determined from spherical cap approximation $R = (d^2 + 4h^2)/8h = 100$ mm[8]. The back focal length (fb) was calculated by the following equation:

$$f_b = n_2 \frac{n_1 R - (n_1 - 1)h}{n_1(n_1 - 1)}$$

The required back focal length is 11 mm. Backward calculations shows that the use of a lens with curvature 4 mm and radius 6 mm will focus the fluorescent probes sufficiently for reliable phototransistor detection and amplify the detection sensitivity by the ratio of the new photon accepting area (113.19 mm^2) over the lens-free (17.72 mm^2), nearly 7 fold.

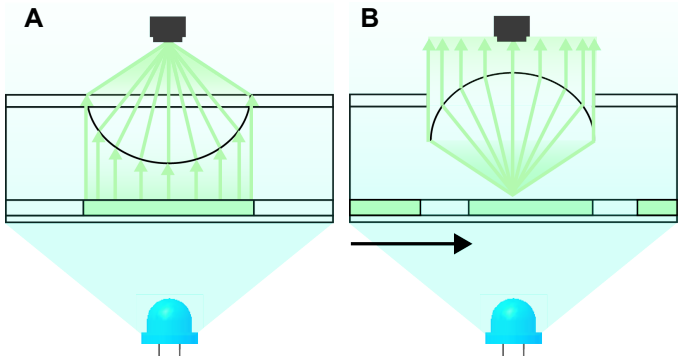

Figure 5 | Two Possible Lens Configurations for Low Intensity and High Specificity Detection. A Lens configuration for low intensity fluorescence detection. Low intensity fluorescence is collected and concentrated on the phototransistor **B** High specificity lens for high-throughput detection. Large arrays of mutations can be processed post-amplification by detecting intensity as different PCR wells pass over a single detector as described by Lim et al[9]. This image is further explained in the Future Work section.

Conclusion

Ultimately, the thermal simulation led to an optimized well geometry of 0.5 mm x 11 mm radius for the pre-concentration well and 0.25 mm x 3.6 mm radius for the allele specific PCR well. Thermal uniformity in the pre-concentration well was 4 °C and 1.5 °C in the allele-specific PCR well. Total cycle time for the pre-concentration PCR took 7 minutes and allele-specific PCR took 5 minutes.

Overall device run-time is roughly 30 minutes from placement of sample, which is an improvement over the reference device by roughly 20 minutes using the same simulation model.

Optical calculations determined that a safe minimum for signal detection was 3.4 pM concentration of scorpion probe. This small detection requirement is much lower than standard scorpion probe use, making the optical detection much less concerning as an optimization factor.

Future Work

Though the current optimized chip is specialized for five specific mutations related to cancer treatment, it is still possible to improve the device by creating a highly multiplexed device. Such a device would have many more mutations tested on smaller sample volumes, and as a result a smaller feasible well depth (0.05 - 0.1 mm height). The consequences of such a device would be much more uniform heating and cooling and reduced cycle duration.

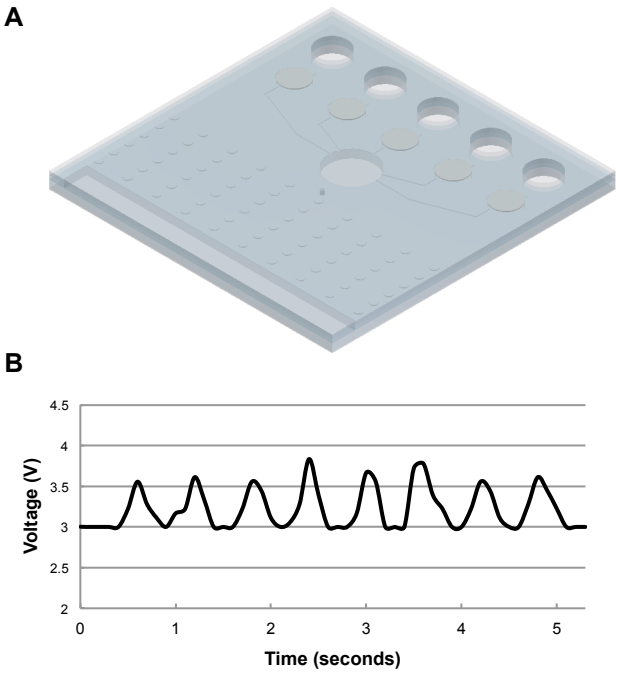

Figure 6 | High Throughput Device and Expected Signal Output. A High throughput device with same inlet and pre-concentration configuration, but with many more mutation specific wells **B** Possible signal output from high-throughput chip sliding over row of LED-phototransistor pairs.

A modification to a high-throughput chip detection process is described earlier in **Figure 5B** as a concave lens configuration for increased sensitivity. The presented device autonomously slides the chip after amplification to another part of the housing where each well is between an LED-phototransitor pair. Using the configuration in **Figure 5B**, which has much greater spatial resolution, a high throughput chip could be slid over a row of LED-phototransistor pairs which would collect data for each well as the well slid past as predicted in **Figure 6B**.

Received 14 May; Accepted 14 May 2014.

1. Hoxha, O. Multiplexed, Single Step, On Chip Mutation Detection in Circulating Tumor DNA Device. (Unpublished)
2. Unpublished.
3. E. K. Wheeler, C. A. Hara, J. Frank, J. Deotte, S. B. Hall, W. Benett, C. Spadaccini and N. R. Beer. Under-three minute PCR: Probing the limits of fast amplification. Analyst 136, 3707-3712 (2011).
4. Yung T. K., Chan K. C., Mok T. S., Tong J., To K. F., Lo Y.M. Single molecule detection of epidermal growth factor receptor mutations in plasma by microfluidics digital PCR in non-small cell lung cancer patients. Clin Cancer Res. 15(6):2076-84(2009)
5. Part Number OP805TXV-ND. DigiKey Electronics. http://www.digikey.com/product-detail/en/OP805TXV/OP805TXV-ND/1636766
6. Whitesides G. M. and Tang, S.K.Y. Fluidic Optics. Keynote, Department of Chemistry and Chemical Biology, Harvard. https://gmwgroup.harvard.edu/pubs/pdf/971.pdf
7. Lee, T. et al. Development of a Fully Automated and Controlled Host Unit for the Detection and Monitoring of Genetic Mutations in Circulating Tumor DNA (Unpublished)
8. M. He, X.-C. Yuan, N. Q. Ngo, J. Bu and V. Kudryashov, Opt. Lett., 2003, 28, 731.
9. Lim, J., Gruner, P., Konrad, M., Baret J-C. Micro-optical lens array for fluorescence detection in droplet-based microfluidics. Lab Chip. 13, 1472-1475 (2013).
10. Material: PDMS (polydimethylsiloxane). MIT Material Property Database. http://www.mit.edu/~6.777/matprops/pdms.htm
11. Material: PMMA. MIT Material Property Database. http://www.mit.edu/~6.777/matprops/pmma.htm

Acknowledgements This project would not have been possible without the support of the University of California, Berkeley Bioengineering Department and professor Luke Lee.

Author Contributions Ori Hohxa et al developed the original on-chip device, Taylor Lee developed the device housing unit, and Amanda Haack determined the biological requirements for the device.